Electric Birefringence of Polystyrene around the Glass Transition Zone

Tadashi Inoue,* Hidenori Kadoya, and Takayuki Onogi

Institute for Chemical Research, Kyoto University, Uji, Kyoto 611-0011, Japan

Received June 9, 2003; Revised Manuscript Received July 19, 2003

ABSTRACT: Electric birefringence (Kerr effect) of polystyrene melts (molecular weight 10 500 and 1050) was measured under low electric field in the frequency range $0.1-10^5$ Hz at various temperatures near and above the glass transition temperature. Frequency−temperature superposition was applicable to obtain a composite curve. A weak dispersion of the complex Kerr coefficient was observed in the glass transition zone of the viscoelastic relaxation spectrum. The time evolution of the electric birefringence was found to be in accord with the relaxation of the "strain-induced" birefringence originated by main-chain orientation after step strain.

Introduction

Polymeric materials become anisotropic and birefringent when they are subjected to external fields such as strain field, electric field, and magnetic field.[1] For the case of polymer melts, the strain-induced birefringence can be related to the stress through the stress−optical rule (SOR).[2] The validity of the SOR indicates that the molecular origin of the stress and birefringence is the orientation of the main chain. On the other hand, for glassy polymers, the SOR does not hold. This comes from that the stress and the birefringence of glassy polymers cannot be simply related to main-chain orientation. Recently, we found that the strain-induced birefringence of amorphous polymers can be related with the stress *quantitatively* through the modified stress−optical rule (MSOR) over a wide time region covering the terminal flow region to the glassy zone in the viscoelastic relaxation spectrum.[3] The MSOR says that both the stress and birefringence have two molecular origins, the R and G components: The R component is originated by main-chain orientation, and the G component is originated by the glassy nature of amorphous polymers. The R component is well described with the bead−spring theory, and it may be called "polymeric" mode. The usage of the MSOR is that the relaxation of the chain orientation is quantitatively evaluated by simultaneous measurements of the stress and birefringence.

Electric birefringence (Kerr effect) has been used to investigate structure and dynamics of polymeric systems.[1] The Kerr coefficient of polymers being measured under the steady state of electric field has been utilized to examine molecular theories for chain conformations. The rotational isomeric state model provides a satisfactory estimation of the Kerr coefficient of polymers.[4,5]

The transient response for the Kerr effect has been studied theoretically by using the "polarizable dipolar molecule" model.[6−8] According to these studies, the Kerr effect rise and decay response functions respectively subjected to step-on and step-off electric fields are equivalent for the induced dipole moment contribution, while the corresponding functions are not equivalent for the permanent dipole moment contribution. Consequently, the complex Kerr coefficient obtained by using the oscillatory field is, in general, not a simple Fourier transformation of the rise or decay function not like mechanical or dielectric cases. The decay function can be expressed in terms of the field-free angular correlation functions.[8] Thus, the transient response of Kerr effect measurements can probe molecular motions of bulk polymers. Beevers et al. measured the electric birefringence of poly(phenylmethylsiloxane), PPMS,[9] and poly(propylene glycol)[10] near their glass transition temperature. For the case of PPMS, they found that the Kerr effect and dielectric relaxations are broader than the single relaxation time process and that $\tau_{K,r} < \tau_{K,d} < \tau_\epsilon$ and $\beta_{K,r} < \beta_{K,d} < \beta_\epsilon$, where subscripts K,r; K,d; and ϵ refer to Kerr effect rise, decay, and dielectric, respectively; τ and β are the relaxation time and the Williams−Watts relaxation parameter, respectively. They suggested that the observed Kerr effect is largely due to the motion of the phenyl group about the bond joining the silicon atom to the aromatic ring. On the other hand, for the case of poly(propylene glycol), two relaxation processes were observed: a fast primary process associated with a negative birefringence and a slow secondary process associated with a positive birefringence. From a comparison with dielectric measurements, they concluded that these measurements are probing effectively different aspects of the same molecular motions. The secondary process showed greatly molecular weight dependence and therefore is related to global motions of the chain. The transient Kerr response of poly(methyl methacrylate) in the glassy state and its temperature dependence were investigated.[11,12] The response consisted of two components, which could be attributed to the α- and β-relaxations.

It should be noted that the above published data on bulk polymers are limited to polymers having the permanent dipoles. Stockmayer and Baur calculated the relaxation of Kerr effect of flexible polymers at low field level with the Zimm model.[13] They showed that if the permanent dipole contribution can be ignored, the imaginary part of the complex Kerr coefficient is proportional to the imaginary part of the complex shear modulus. However, this prediction has not been experimentally examined. In the present study, we report the electric birefringence data of polystyrene melts around the glass transition zone and compare them with viscoelastic data. For the case of polystyrene, it is known that contribution of the permanent dipole to the Kerr coefficient is negligibly small.[5,14,15] Therefore, we an-

* To whom all correspondence should be addressed.

10.1021/ma0303162 CCC: $25.00
Published on Web 11/20/2003

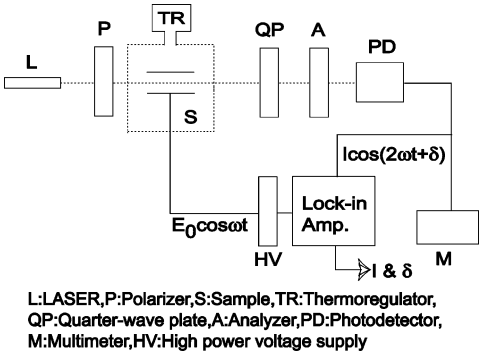

Figure 1. Apparatus for electric birefringence measurements.

Table 1. Polystyrene Samples and Basic Parameters

code	M_w/kg mol^{-1}	M_w/M_n	T_g/K	T_r/K
A1000	0.105	1.2	282.0	298.2
F1	1.05	1.02	367.0	379.2

ticipate a good correspondence between the viscoelasticity and the electric birefringence for PS considering the Stockmayer and Baur theory. As described above, for the case of polymer melt viscoelasticity, the glassy component contributes to the stress at short times. We will separate the modulus into the polymeric and the glassy modes with the MSOR and compare the Kerr coefficient and the polymeric mode.

Experimental Section

Samples. Low molecular weight polystyrenes, A1000, and F1 were purchased from Toso Co. Ltd. All samples were used without further purification. The molecular weight and polydispersity index are provided in Table 1.

Apparatus. Figure 1 illustrates the experimental apparatus for the electric birefringence measurements. The laser beam from a He−Ne laser ($\lambda = 632.8$ nm) is incident to a Kerr cell through the Gran-Tayler polarizer. The beam is detected through a quarter wave plate and an analyzer. Two types of cells having different optical path ($l = 10$ and 50 mm) were used. The signal from the lock-in-amplifier (Stanford Research, SR 820) or function generator (NF, wave factory) is amplified with a power amplifier (NF, HVA 4321). The operating electric field was typically 100 kV m^{-1}. The frequency range of the electric field is 0.1 Hz−50 kHz.

For detection of very low birefringence, Δn, we followed the method by Ookubo et al.[16] The analyzer was set with a small offset angle α from its extinction angle. The light intensity I after the analyzer is given by

$$I/I_0 = \sin\left(\frac{\pi l \Delta n}{\lambda}\right) \sin\left(\frac{\pi l \Delta n}{\lambda} + 2\alpha\right) + \sin^2 \alpha \qquad (1)$$

Here, I_0 is the intensity of the incident light. Equation 1 can be written for $\pi l \Delta n/\lambda \ll a \ll 1$

$$I/I_0 = \frac{\pi l \Delta n}{\lambda} \alpha + \alpha^2 \qquad (2)$$

The complex Kerr coefficients, K_{DC}, K', and K'' are calculated from in-phase and out-phase components at frequency 2ω.

$$K \equiv \frac{\Delta n}{E^2} = K_{DC} + \mathrm{Re}[(K' - iK'') \exp(-i2\omega t)] \qquad (3)$$

Here, E is the magnitude of the electric field.

For measurement of DC component of the Kerr coefficient, K_{DC}, we applied the amplitude modulation method (AM method). In the AM method, the amplitude of the electric field is varied sinusoidally.

$$E = E_0(1 + \cos \Omega t) \sin \omega t \qquad (4)$$

Since Ω should be larger than ω, measurement of K_{DC} was limited $10 < \omega/s^{-1} < 10\,000$. Over a whole frequency region, K_{DC} was approximately constant, which is in accord with Tonelli's calculation that the contribution of permanent dipole is negligibly small.[14]

Measurements were performed at isothermal conditions at several temperatures. For each measurement, temperature was slowly decreased from a higher temperature and kept at desired temperature for enough long time (typically 1 day) to minimize the residual birefringence. All measurements were performed above the glass transition temperature. Data measured with different combination of Kerr cell and thermojackets (homemade heater block and Optistat DN, Oxford) agreed with each other within experimental accuracy. This convinced us that the effect of residual and parasite birefringence is negligible.

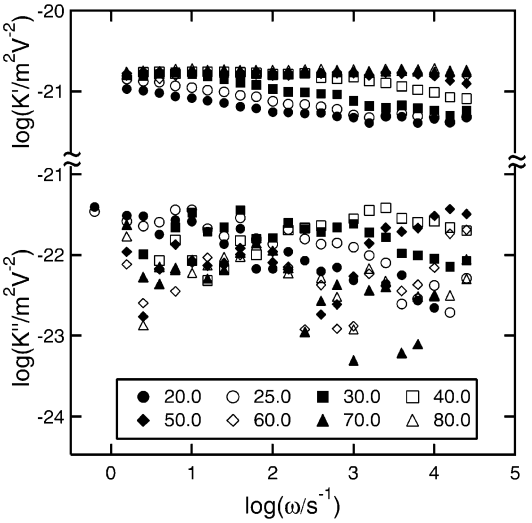

Figure 2. Frequency dependence of the complex Kerr coefficient, K^*, for A1000. Numbers in legend represent temperature in centigrade.

Results

The complex Kerr coefficients, $K'(\omega)$ and $K''(\omega)$, for A1000 at various temperature are plotted against frequency in Figure 2. At the highest temperature, 80 °C, $K'(\omega)$ varies little with frequency and the value is about 1.8×10^{-21} m^2 V^2. At this temperature, $K''(\omega)$ is more than 10 times smaller than $K'(\omega)$. At lower temperatures, $K'(\omega)$ decreases with increasing frequency, and the maximum of $K''(\omega)$ can be seen in the middle of the frequency range at 30 °C.

Motivated by the time−temperature superposition principle for polymer melt rheology, we constructed the composite curves from the data shown in Figure 2 with the method of reduced variables: $K'(\omega)$ and $K''(\omega)$ data plotted against ω in double-logarithmic scales at each temperature were shifted along the abscissa. The results are shown in Figure 3. The shift factor for horizontal shifts, a_T, was determined so that the best superposition was obtained for K'. The temperature dependence of a_T will be discussed later. The superposition was fairly well. Here, we did not use vertical shifts. According to theories for electric birefringence, the Kerr coefficient originated by the induced dipoles is inversely proportional to temperature, T, if the anisotropy of polariz-

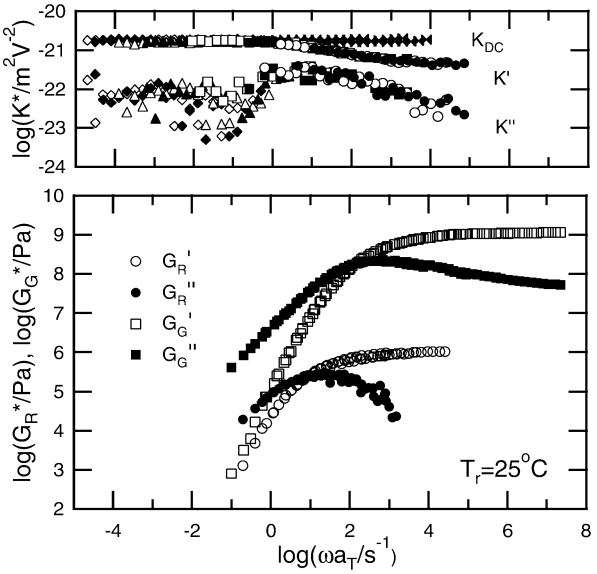

Figure 3. Composite curve for the complex Kerr coefficient, K^*, for A1000 (upper panel). Symbols are same as Figure 2. For comparison, the complex shear modulus, the R and G components of the shear modulus are presented (lower panel).

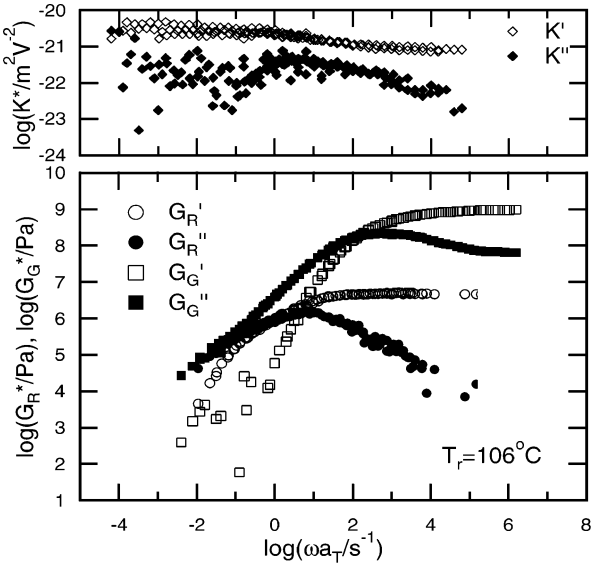

Figure 4. Composite curve for the complex Kerr coefficient for F1 (upper panel). For comparison, the R and G components of the shear modulus are presented (lower panel).

ability is independent of temperature.[13] This is because the orientation induced by the electric field is agitated by thermal motions. We examined this theoretical vertical shift. However, the procedure did not provide better results, and therefore we decided to ignore the vertical shift. Since the temperature range of the data displayed here is from 20 to 80 °C, the maximum error due to ignoring the vertical shift is less than 20%.

Relaxation of K' is observed at frequencies $1 < \log(\omega/s^{-1}) < 3$. This means that the orientation of the chain can follow the field only at low frequencies. Also included is the DC component of Kerr coefficient, K_{DC}. K_{DC} was independent of frequency, which supports that induced dipoles are main origin of the Kerr effect of PS. The permanent dipole cannot follow the inversion of electric field without molecular reorientation, and therefore the DC component decreases if the frequency of the electric field exceeds the rate of molecular motions.[1]

To discuss the relationship between the electric birefringence and viscoelasticity, G^* data are displayed in Figure 3. G^* for A1000 is typical for low molecular weight glass-forming materials: No significant polymeric modes like the Rouse modes ($G' = G' \propto \omega^{0.5}$) are observed because the molecular weight is comparable to the Rouse segment size. To estimate the polymeric mode, we applied the modified stress−optical rule to the G^* together with strain−birefringence coefficient.[3] According to the MSOR, the modulus and strain−optical coefficient, B^* ($= \Delta n^*/\gamma$), can be related with each other through the two component functions, G_R^* and G_G^*.

$$G^* = G_R^* + G_G^* \tag{5}$$

$$B^* = C_R G_R^* + C_G G_G^* \tag{6}$$

Here C_R and C_G are the stress−optical coefficients associating the R and G components. The R component, G_R^*, is related to chain orientation and may be called polymeric mode, and the G component, G_G^*, is to the glassy properties. Details of the separation into the two component functions by the MSOR are described in a previous paper.[17] The results are presented in Figure 3. The estimated polymeric mode, G_R^*, was very weak, and G_G^* is approximately the same as G^*. It should be noted that the shape of $\log(G_R''/\text{Pa})$ is very similar to $\log K''(\omega)$ around $1 < \log \omega < 2$. The similarity strongly suggests that the relaxations of both quantities are originated by the same molecular process.

Molecular Weight Dependence. Similar results were obtained for F1 having a higher molecular weight. Figure 4 shows results for F1. Here, the reference temperature is chosen so that location of G_G'' at the frequency axis agrees between Figures 3 and 4. For the case of F1, G_R^* is significant. The shape of $\log(G_R''/\text{Pa})$ is very similar to $\log K''(\omega)$ as the case of A1000. The relative position of G_R'' to G_G'' changes with molecular weight: The maximum of G_R'' locates at lower frequencies than that for A1000. With increasing molecular weight, the maximum of K'' also slightly shifts to lower frequencies. Thus, the similarity between $\log(G_R''/\text{Pa})$ and $\log K''(\omega)$ holds well for the two samples.

Relationship between Electric Birefringence and Modulus. To test the relaxation between G_R'' and $K''(\omega)$, a detailed comparison of G_R'' and $K''(2\omega)$ is shown in Figure 5. Agreement between $\log(G_R''/\text{Pa})$ $\log K''(2\omega)$ holds well over a wide frequency region. This means the following relationship holds well.

$$K''(2\omega) \propto G_R''(\omega) \tag{7}$$

At high frequencies, the proportionality between G_R'' and K'' is not so good. This would be due to an insignificant but nonnegligible contribution of the glassy component to the Kerr coefficient. According to the molecular interpretation of the MSOR, the strain-induced birefringence can be related to the longitudinal and transverse anisotropy of the repeating unit.[17]

$$\Delta n = \Delta\alpha P_R + \Delta\alpha_T P_G \tag{8}$$

Here, P_R and P_G are orientation functions representing orientation of the main-chain axis and twisting of the repeating units about the main-chain axis. Δa_T and Δa_T

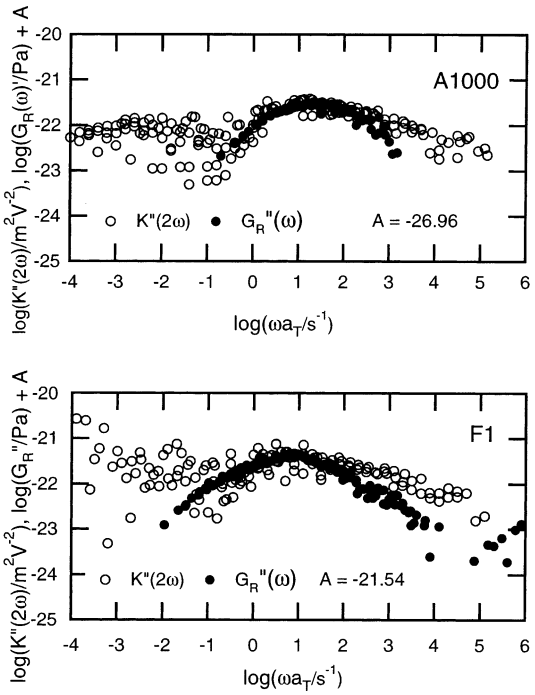

Figure 5. Comparison of $K''(2\omega)$ and $G_R''(\omega)$.

are respectively longitudinal and transverse anisotropies defined as follows.

$$\Delta\alpha = \alpha_X - \frac{\alpha_Y + \alpha_Z}{2} \tag{9}$$

$$\Delta\alpha_T = \frac{\alpha_Y - \alpha_Z}{4} \tag{10}$$

Δa_T can orient the repeating units and cause birefringence. It should be remarked that twisting of the repeating unit would require large energy as expected from that the G component has a high glassy modulus. Thus, we expect that the G component requires 2 order larger torques to cause the same order of birefringence because G_G' is larger than G_R' by a factor of 100. Thus, we may conclude that the electric birefringence is mainly caused by the chain orientation in contrast to the strain-induced birefringence.

Temperature Dependence. Figure 6 shows a comparison of temperature dependence of the Kerr coefficient and the viscoelastic functions. At high temperatures, the temperature dependence of K^* is close to that for the R component. This result also supports that the main part of the birefringence is originated by the chain orientation. At low temperatures, the temperature dependence of K^* is similar to that for the G component. This result suggests the significant contribution of the G component to the Kerr coefficient.

Discussion

Electric birefringence of the beads−springs model was calculated by Stockmayer and Baur.[13] Here we briefly describe their calculation. The reader is assumed to be familiar with the work of Zimm.[18] We ignored contribution of permanent dipole. The electric force acting the ith bead may be given by

$$3F^3(\alpha_1 - \alpha_2)(2x_i - x_{i+1} - x_{i-1})/5b^2 \tag{11}$$

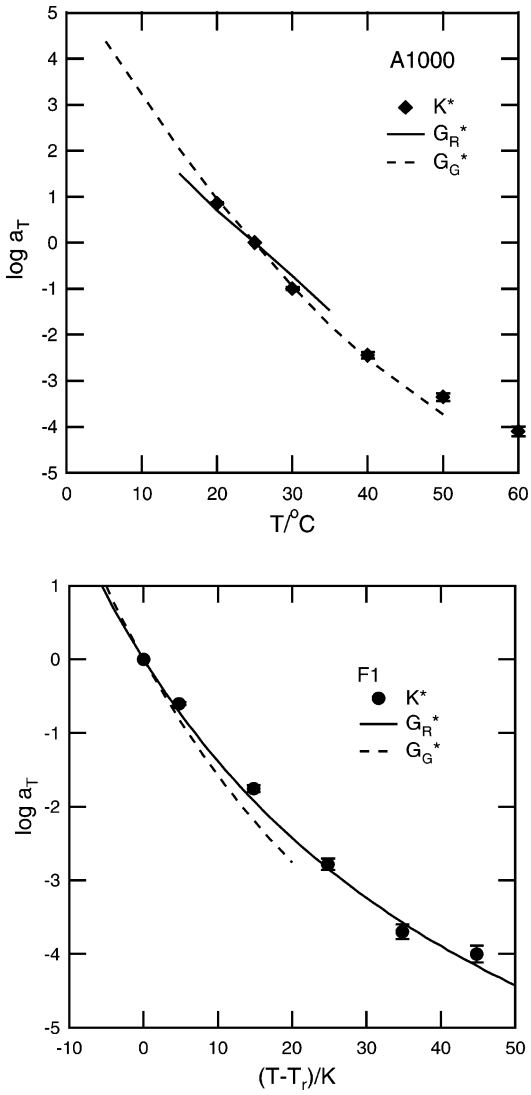

Figure 6. Temperature dependence of shift factors for Kerr coefficient and viscoelastic functions.

Here, F is local field $F = E(\epsilon + 3)/3$ and E is unidirectional electric field pointing along the x-direction. $\alpha_1 - \alpha_2$ is the anisotropy of polarizability of the beads. The resulting diffusion equation is

$$\frac{\partial\psi}{\partial t} = \left(\frac{\partial}{\partial \mathbf{x}}\right)^T\left[D\mathbf{H}\left(\frac{\partial\psi}{\partial \mathbf{x}}\right) + \sigma(1 - \beta^2F^2q^2)\mathbf{HAx}\psi\right] \tag{12}$$

Here, D is diffusion coefficient of beads, β is $1/kT$, and q^2 is $(\alpha_1 - \alpha_2)/5\beta$. Equation 12 can be solved by the perturbation calculation. Solving eq 12 to the second-order perturbations in the field, we have the following equation for decay of the birefringence from the steady state.

$$\frac{\Delta n(t)}{E^2} = K_{sp}\sum_k \varphi_k(t)^2 \tag{13}$$

$$\varphi_k(t) = \exp\left(-\frac{t}{2\tau_k}\right) \tag{14}$$

Here, τ_k agrees with viscoelastic relaxation time of the Zimm model

$$G(t) = G\sum_k \exp\left(-\frac{t}{\tau_k}\right) \tag{15}$$

and can be determined from eigenvalue for the Rouse−Zimm matrix, λ_k

$$\tau_k = \frac{\lambda_k}{2kT} \tag{16}$$

Since φ_k appears squared in eq 13, the relaxation times of birefringence agree with those for modulus. Thus, the relaxation of the electric birefringence from the steady state agrees with the stress−relaxation process.

For the oscillatory electric field, the birefringence can be written as follows.

$$\Delta n = \frac{{E_0}^2 B}{2}\left[1 + \sum_k \frac{1}{1 + (2\omega\tau_k)^2}\cos 2\omega t + \sum_k \frac{2\omega\tau_k}{1 + (2\omega\tau_k)^2}\sin 2\omega t\right] \tag{17}$$

Since the complex shear modulus of the Zimm model can be written as follows

$$G_{BS}^* = G'_{BS} + iG''_{BS} = \sum_k \frac{(\omega\tau_k)^2}{1 + (\omega\tau_k)^2} + i\sum_k \frac{\omega\tau_k}{1 + (\omega\tau_k)^2} \tag{18}$$

we obtain the relationship

$$K''(2\omega) = G''_{BS}(\omega) \tag{19}$$

Equation 19 agrees with the present experimental result, eq 6.

A comment may be needed on the molecular weight range where eq 19 holds well. In a previous study, we studied viscoelasticity of a series of low molecular polystyrenes, and we showed that G_R^* for F1 can be described with the Rouse model with 12 modes.[19] Therefore, the validity of eq 19 may be reasonable. On the other hand, for the case of A1000, the whole chain size is comparable to one segment size, $M \sim 850$. For such a low molecular weight system, the validity of the beads−spring models is still open to question. However, it may be worthwhile to note that, for the case of rodlike polymers having induced dipole, eq 19 holds well in the dilute regime. Thus, we believe that the relationship eq 19 would have phenomenological universality.

Concluding Remarks

Electric birefringence (Kerr effect) of polystyrene, for which the effect of permanent dipole is negligible, has been measured in linear region (low electric field) around the glass transition zone. The imaginary part of the complex Kerr coefficient is proportional to the imaginary part of the R component, G_R^*, which represents contribution of main-chain orientation to the whole modulus. The present result means that the time evolution of the electric birefringence originated by induced dipole is described with the relaxation of the strain-induced birefringence originated by main-chain orientation after step strain. Thus, the response of polymer chain to the strain field and electric field can be described consistently. The modification of Zimm theory by Stockmayer and Baur describes the feature of experimental results.

Recently, manipulation of polymeric materials by using magnetic fields is anticipated to be a new polymer processing method. The effects of the magnetic field on crystallization of polymers have been studied.[20] It may be worthwhile to note that orientation of polymeric chain in the magnetic field can be expressed by the analogy of eq 19. We predict that the time dependence of orientation in the magnetic field also would be described by G_R^*.

Acknowledgment. This study was partially supported by a Grant-in-Aid for Scientific Research (No. 13450391 and 13650952) from the Ministry of Education, Culture, Sports, Science, and Technology of Japan.

References and Notes

(1) Riande, E.; Saiz, E. *Dipole Moment and Birefringence of Polymers*; Prentice Hall: New York, 1992.
(2) Janeschitz-Kriegl, H. *Polymer Melt Rheology and Flow Birefringence*; Springer-Verlag: Berlin, 1983.
(3) Inoue, T.; Okamoto, H.; Osaki, K. *Macromolecules* **1991**, *24*, 5670.
(4) Flory, P. J. *Statistical Mechanics of Chain Molecules*; John Wiley & Sons: New York, 1969.
(5) Mattice, W. L.; Suter, U. W. *Conformational Theory of Large Molecules; The Rotational Isomeric State Model in Macromolecular Systems*; Wiley: New York, 1994.
(6) Benoit, H. *J. Chim. Phys. Phys.-Chim. Biol.* **1952**, *49*, 517.
(7) Beevers, M. S.; Crossley, J.; Garrington, D. C.; Williams, G. *J. Chem. Soc., Faraday Trans. 2* **1976**, *72*, 1482.
(8) Rosato, V.; Williams, G. *J. Chem. Soc., Faraday Trans. 2* **1981**, *77*, 1767.
(9) Beevers, M. S.; Elliott, D. A.; Williams, G. *Polymer* **1980**, *21*, 279.
(10) Beevers, M. S.; Elliott, D. A.; Williams, G. *Polymer* **1980**, *21*, 13.
(11) Jungnickel, B.-J. *Polymer* **1981**, *22*, 720.
(12) Ullrich, K.; Jungnickel, B.-J. *Eur. Polym. J.* **1985**, *21*, 991.
(13) Stockmayer, W. H.; Baur, M. E. *J. Am. Chem. Soc.* **1964**, *86*, 3485.
(14) Tonelli, A. E. *Macromolecules* **1977**, *10*, 153.
(15) Khanarian, G.; Cais, R. E.; Kometani, J. M.; Tonelli, A. E. *Macromolecules* **1982**, *15*, 866.
(16) Ookubo, N.; Hirai, Y.; Ito, K.; Hayakawa, R. *Macromolecules* **1989**, *22*, 1359.
(17) Inoue, T.; Onogi, T.; Osaki, K. *J. Polym. Sci., Part B: Polym. Phys.* **2000**, *38*, 954.
(18) Zimm, B. H. *J. Chem. Phys.* **1956**, *24*, 269.
(19) Inoue, T.; Onogi, T.; Osaki, K. *J. Polym. Sci., Polym. Phys. Ed.* **1999**, *37*, 389.
(20) Ezure, H.; Kimura, T.; Ogawa, S.; Ito, E. *Macromolecules* **1997**, *30*, 3600.

MA0303162